

### 33. Structural and Spectroscopic Investigations of the 1:1 Complex between Europium Nitrate and a Tetraoxadiaza Macrocycle<sup>1)</sup>

by Jean-Claude G. Bünzli\*, Gordon A. Leonard, and Dominique Plancherel

Institut de chimie minérale et analytique, Université de Lausanne, Place du Château 3, CH-1005 Lausanne

and Gervais Chapuis

Institut de cristallographie, Université de Lausanne, BSP, CH-1015 Lausanne

(25.XI.85)

The crystal and molecular structure of dinitrato(1,7,10,16-tetraoxa-4,13-diazacyclooctadecane)europium(III) nitrate,  $[(\text{Eu}(\text{NO}_3)_2(\text{C}_{12}\text{H}_{26}\text{N}_2\text{O}_4)]\text{NO}_3$  has been determined from single-crystal X-ray diffraction:  $a = 12.567(3)$ ,  $b = 11.585(3)$ ,  $c = 16.354(5)$  Å,  $\beta = 112.45(2)^\circ$ , space group  $P2_1/n$ ,  $Z = 4$ . The structure consists of discrete dinitrato complex cations and of nitrate anions. The Eu(III) ion is 10-coordinate, bonding to the six donor atoms of the macrocycle and to four O-atoms of the two bidentate nitrates. The mean distances are  $\text{Eu}-\text{O}(\text{ether}) = 2.60(2)$ ,  $\text{Eu}-\text{O}(\text{NO}_3) = 2.47(3)$  and  $\text{Eu}-\text{N} = 2.62(2)$  Å. The metal site has an approximate  $C_2$  symmetry. The IR and Raman spectra show the presence of an ionic and of two bonded bidentate nitrates. These latter have a different  $\nu_1-\nu_4$  splitting, which reflects their dissymmetrical bonding. Luminescence spectra have been recorded at 296, 77, and 4 K by laser-excitation techniques. One sharp  ${}^3\text{D}_0 \leftarrow {}^7\text{F}_0$  transition was observed and almost all the sublevels of the  ${}^7\text{F}_J$  manifold could be identified. The interaction between a sharp distribution of the phonon states (especially between 950 and 1200  $\text{cm}^{-1}$ ) and the electronic  ${}^7\text{F}_2$  sublevels results in the presence of several satellite lines accompanying the  ${}^5\text{D}_0 \rightarrow {}^7\text{F}_2$  transition. In MeCN solutions, both luminescence and conductivity data point to the presence of the  $[\text{Eu}(\text{NO}_3)_2(2,2)]^+$  cation.

**Introduction.** – Synthetic ionophores are being increasingly used to study the coordination chemistry of lanthanide ions [2] [3]. The 18-membered ligand 1,7,10,16-tetraoxa-4,13-diazacyclooctadecane (2,2) is the basic unit of a class of tricyclic compartmental cryptands used to bind organic [4] or metal [5] cations. The presence of the two amine groups has a stabilizing influence, and lanthanide complexes with this ligand are approximately three orders of magnitude more stable than corresponding complexes with the cyclic hexaether 18-crown-6 [2] (1,4,7,10,13,16-hexaoxacyclooctadecane). No structural data are available for lanthanide coronates with the ligand (2,2), and it is not known if these compounds are simple neutral 1:1 complexes, or if they contain cationic species of the type  $[\text{LnX}_2\text{L}]^+$  similar to those observed in complexes of 18-crown-6 ether with lanthanide nitrates [6] [7] or chlorides [8].

As part of our work on macrocyclic complexes, we report the crystal structure determination of the 1:1 complex between europium(III) nitrate and the ligand (2,2), along with a discussion of the nitrate vibrational modes.

The use of trivalent lanthanide ions to probe the metal-ion binding sites of ionophores is well-established [2], particularly in conjunction with laser-luminescence techniques. To set a basis for further studies on dinuclear cryptands [5], we also report the low-temperature emission spectrum of the complex with ligand (2,2).

<sup>1)</sup> Part 26 of the Series 'Complexes of Lanthanoid Salts with Macrocyclic Ligands'; Part 25: [1].

**Experimental.** - Preparation of  $\text{Eu}(\text{NO}_3)_3 \cdot (2,2)$ . The complex was prepared in anh. MeCN as described in [9], using *Kryptofix 22* from *Merck*. Suitable monocrystals were grown by slow evaporation of an MeCN soln. Their composition and purity were ascertained by elemental analysis.

**Spectroscopic Measurements.** IR spectra were obtained as nujol mulls and KBr pellets with a *Perkin-Elmer* model 577 and an *IFS-113v Bruker* FT-IR spectrometers. Raman spectra of powdered samples were recorded on a *Ramalog-4* spectrometer from *Spex Industries Inc.* Luminescence spectra of polycrystalline samples (296, 77, and 4 K) and of MeCN solns. (296 K) were recorded on a laser spectrofluorimeter described in [10]. Conductivity measurements were obtained with a *Metrohm E-365B* conductometer equipped with an *EA-655* cell; the  $\text{H}_2\text{O}$  content of the MeCN solns. was lower than 60 ppm, corresponding to less than 2-3 molecules of  $\text{H}_2\text{O}$  per  $\text{Eu}^{3+}$ .

**Collection of the X-Ray Diffraction Data.** A crystal of dimension  $0.26 \times 0.27 \times 0.22$  mm was sealed under Ar atmosphere and data were collected at r.t. on a *Syntex P<sub>2</sub>* four-circle diffractometer using Nb-filtered  $\text{MoK}_\alpha$  radiation. The background noise and variance of each reflection were calculated using the *Lehman-Larsen* algorithm [11]. Three standard reflections were measured every 100 reflections and showed a slight variation in intensity which was corrected for. The data were also corrected for *Lorentz*, polarization and absorption effects. In total 3955 data reflections were measured, 2898 were unique and 2531 were considered to be observed ( $I/\sigma(I) \geq 3$ ). Systematic absences were of the form  $0k0:k \neq 2n$  and  $h0l:h + l \neq 2n$  uniquely defining the space group  $P2_1/n$  (ITC No. 14). Unit cell dimensions and space group symmetry were subsequently confirmed by precession photographs.

**Crystal Data.**  $\text{C}_{12}\text{H}_{26}\text{N}_5\text{O}_{13}\text{Eu}$ ,  $M = 600.31$ , monoclinic,  $a = 12.567(3)$ ,  $b = 11.585(3)$ ,  $c = 16.354(5)$ , Å,  $\beta = 112.45(2)^\circ$ ,  $U = 2200(2)$  Å<sup>3</sup>, space group  $P2_1/n$ ,  $Z = 4$ ,  $D_c = 1.811$ ,  $D_m = 1.812(4)$  g·cm<sup>-3</sup>,  $F(000) = 1200$ ,  $\mu(\text{MoK}_\alpha) = 29.23$  cm<sup>-1</sup>.

**Structure Determination and Refinement.** The structure was determined by the heavy-atom method, and the assignment of the coronand N-atoms was based on the geometry of the macrocycle. A series of refinements with anisotropic thermal parameters reduced the conventional  $R$  factor ( $= \Sigma(|F_o| - |F_c|)/\Sigma|F_o|$ ) to 0.055.

Examination of a difference *Fourier* synthesis at this stage revealed the presence of residual densities in the vicinity of the ionic nitrate group, indicating positional disorder. A further problem were the lengths and ranges of the C-C (1.37-1.54, mean 1.48 Å), C-O (1.44 1.57, 1.49 Å), and C-N (1.44 1.52, 1.48 Å) distances. This is due to an inadequate treatment of curvilinear vibrations [12] [13], and we, therefore, introduced soft constraints [14] on the distances and angles with weights equal to the inverse of the e.s.d.'s of the prescribed values. Specified distances and angles were 1.52 Å (C-C), 1.42 Å (C-O), and 1.48 Å (C-N), 109.5° (X-C-C), and 113° (C-X-C), X = O or N. The ionic nitrate was also included in the soft-constrained refinement with prescribed values of 1.24 Å (N-O) and 120.0° (O-N-O). The standard deviations of the prescribed values were set to 0.0005 Å (distances) and 0.05° (angles). The H-atoms were generated geometrically and assigned a common isotropic temp. factor,  $U(\text{eq}) = 0.10$ . A weighting scheme,  $w = 1/\sigma(F^2)$ , was applied and the final refinement yielded  $R = 0.034$ ,  $R_w (= [\Sigma w(|F_o| - |F_c|)^2]/\Sigma w|F_o|^2)^{1/2} = 0.043$ . The goodness of fit including soft restrictions reduced to 4.54 ( $= (\Sigma w(F_o - F_c)^2 + \Sigma w(R_p - R_o)^2)^{1/2}/(n_r + n_s - n_c)$ , with  $R_p$  = prescribed distance or angle,  $R_o$  = observed value,  $n_r$  = number

Table 1. Final Atomic Coordinates for the Non-H-Atoms. Estimated Standard Deviations in Parentheses.

Atom	x	y	z	Atom	x	y	z
Eu(1)	0.05269(3)	0.17164(3)	0.30866(2)	N(4)	-0.1871(6)	0.1566(5)	0.2816(5)
C(1)	-0.0388(5)	0.4548(5)	0.3286(3)	N(5)	0.2716(4)	0.1327(5)	0.9536(4)
C(2)	0.0262(7)	0.4718(4)	0.2682(4)	O(1)	0.0233(5)	0.3673(3)	0.2220(3)
C(3)	0.0694(7)	0.3800(4)	0.1558(4)	O(2)	0.0566(4)	0.1739(3)	0.1516(2)
C(4)	0.0398(8)	0.2736(4)	0.0977(3)	O(3)	0.0995(4)	-0.0223(3)	0.3947(3)
C(5)	0.0326(6)	0.0713(3)	0.1002(3)	O(4)	0.1552(5)	0.1771(4)	0.4796(3)
C(6)	0.0485(5)	-0.0324(4)	0.1603(4)	O(5)	0.2428(4)	0.0920(4)	0.3255(4)
C(7)	-0.0235(4)	-0.1211(4)	0.2653(3)	O(6)	0.2406(4)	0.2747(5)	0.3428(4)
C(8)	0.0874(5)	-0.1269(4)	0.3468(3)	O(7)	0.4013(5)	0.1861(5)	0.3676(6)
C(9)	0.1908(5)	-0.0258(4)	0.4791(3)	O(8)	0.1082(5)	0.1115(4)	0.3486(4)
C(10)	0.1775(7)	0.0759(4)	0.5326(3)	O(9)	-0.1527(4)	0.2094(5)	0.2286(4)
C(11)	0.1391(7)	0.2753(4)	0.5258(3)	O(10)	-0.2879(5)	0.1519(5)	0.2711(6)
C(12)	0.1092(5)	0.3792(4)	0.4646(4)	O(11)	0.3637(5)	0.1834(6)	0.9932(5)
N(1)	0.0073(5)	0.3522(4)	0.3845(3)	O(12)	0.2598(5)	0.0732(6)	0.8878(4)
N(2)	-0.0216(4)	-0.0167(4)	0.2142(3)	O(13)	0.1957(6)	0.1329(9)	0.9844(6)
N(3)	0.2978(5)	0.1854(6)	0.3456(5)				

of reflections,  $n_s$  = number of soft restrictions and  $n_v$  = number of refined parameters). The highest peak in the final difference *Fourier* synthesis ( $1.4 \text{ e}/\text{\AA}^3$ ) was located  $0.90 \text{ \AA}$  from the Eu-Atom.

All calculations were carried out using the XRAY-72 system [15]. The anomalous dispersion coefficients for Eu were taken from *Cromer* and *Lieberman* [16], and the atomic scattering factors of neutral atoms from *Cromer* and *Mann* [17]. The final atomic coordinates for non-H-atoms are given in *Table 1*. The final thermal parameters and the final atomic coordinates for H-atoms are available upon request from *J.-C. B.*

**Results and Discussion.** – *Structural Study.* The crystal contains discrete units held together by *van der Waals* interactions (*Fig. 1*). A noteworthy feature is the presence of dinitrato  $[\text{Eu}(\text{NO}_3)_2(2,2)]^+$  cations and ionic nitrate groups. The Eu(III) ion is 10-coordinate, bonding to the six donor atoms of the macrocycle and to the four O-atoms of the bidentate nitrates. Selected bond lengths and angles are reported in *Table 2* and the complex cation is shown in *Fig. 2*.

Upon complexation, the macrocycle loses its original  $C_{2h}$  symmetry [18] and adopts a boat-like conformation with approximate  $C_2$  symmetry, similar to that displayed by 18-membered cyclic polyethers in neutral nitrate complexes of the type  $[\text{Ln}(\text{NO}_3)_3\text{L}]$  with  $\text{L} = 18\text{-crown-6}$ ,  $\text{Ln} = \text{La}$  [19],  $\text{Nd}$  [20], and  $\text{L} = \text{dicyclohexyl-18-crown-6}$ ,  $\text{Ln} = \text{La}$  [21]. Both N-atoms of the amine groups are  $1.09 \text{ \AA}$  out of the least-squares plane ( $\sigma = 0.53 \text{ \AA}$ ) defined by the macrocycle O-atoms, on the same side as the metal ion which lies at  $0.37 \text{ \AA}$ .

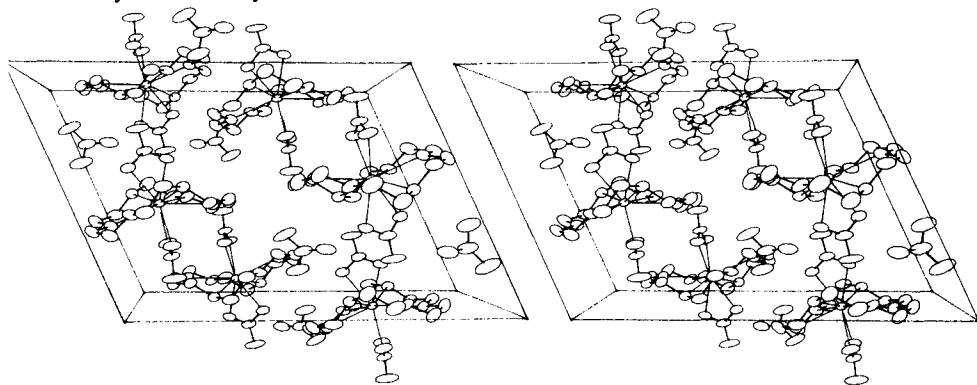


*Fig. 1.* Stereoview of the crystal packing of  $[\text{Eu}(\text{NO}_3)_2(2,2)]\text{NO}_3$

*Table 2.* Selected Bond Lengths [ $\text{\AA}$ ] and Angles [ $^\circ$ ]. Estimated Standard Deviations in Parentheses.

<i>(a) Europium coordination sphere</i>							
Eu–O(1)	2.623(4)	Eu–O(5)	2.477(6)	N(1)–Eu–N(2)	148.5(2)	N(1)–Eu–O(4)	64.9(1)
Eu–O(2)	2.588(5)	Eu–O(6)	2.511(6)	O(1)–Eu–O(3)	175.1(2)	N(2)–Eu–O(2)	64.0(1)
Eu–O(3)	2.597(4)	Eu–O(8)	2.452(7)	O(2)–Eu–O(4)	151.6(2)	N(2)–Eu–O(3)	63.7(1)
Eu–O(4)	2.594(4)	Eu–O(9)	2.447(5)	O(1)–Eu–O(2)	60.5(1)	O(5)–Eu–O(6)	50.7(2)
Eu–N(1)	2.604(5)			O(3)–Eu–O(4)	61.3(1)	O(8)–Eu–O(9)	52.0(2)
Eu–N(2)	2.630(4)			N(1)–Eu–O(1)	63.4(2)		
<i>(b) Bonded nitrates</i>			<i>(c) Organic ligand</i>				
N(3)–O(5)	1.258(8)	O(5)–N(3)–O(6)	116.8(6)	Mean C–C	1.516(2)	Mean C–C–X	109.0(3)
N(3)–O(6)	1.250(9)	O(5)–N(3)–O(7)	120.3(7)	Mean C–O	1.420(1)	Mean C–X–C	112.2(5)
N(3)–O(7)	1.209(9)	O(6)–N(3)–O(7)	122.9(7)	Mean C–N	1.475(1)		
N(4)–O(8)	1.276(8)	O(8)–N(4)–O(9)	115.5(7)	Mean C–H	1.08(7)		
N(4)–O(9)	1.264(11)	O(8)–N(4)–O(10)	123.0(9)	Mean N–H	1.025		
N(4)–O(10)	1.213(9)	O(9)–N(4)–O(10)	122.5(7)				

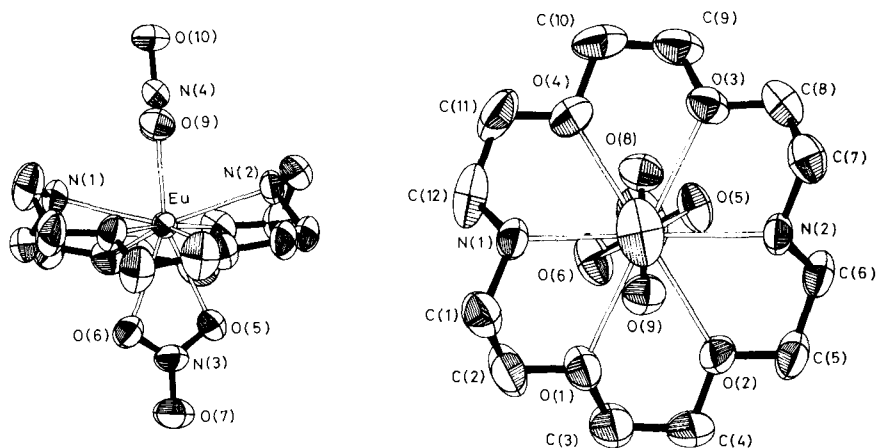


Fig. 2. Structure of the  $[Eu(NO_3)_2(2,2)]^+$  cation showing the 50% probability thermal ellipsoids and the atom-numbering scheme

Table 3. Torsion Angles [ $^\circ$ ] in the Complexed Ligand (2,2)

N(1)–C(1)–C(2)–O(1)	53	O(4)–C(5)–C(6)–N(2)	54	O(3)–C(9)–C(10)–O(4)	-47
C(1)–C(2)–O(1)–C(3)	172	C(5)–C(6)–N(2)–C(7)	172	C(9)–C(10)–O(4)–C(11)	179
C(2)–O(1)–C(3)–C(4)	-168	C(6)–N(2)–C(7)–C(8)	79	C(10)–O(4)–C(11)–C(12)	-177
O(1)–C(3)–C(4)–O(2)	-43	N(2)–C(7)–C(8)–O(3)	55	O(4)–C(11)–C(12)–N(1)	56
C(3)–C(4)–O(2)–C(5)	-179	C(7)–C(8)–O(3)–C(9)	171	C(11)–C(12)–N(1)–C(1)	171
C(4)–O(2)–C(5)–C(6)	-178	C(8)–O(3)–C(9)–C(10)	-166	C(12)–N(1)–C(1)–C(2)	85

In the other complexes for which a crystal structure has been reported, the metal ion has usually been found in the center of the (2,2) cavity [22]. For instance, the complex with potassium thiocyanate is comprised of  $[K(2,2)]^+$  cations with  $C_{2h}$  symmetry in which the ligand displays the chair conformation. The N-atoms are 0.64 Å above and under the plane of the O-atoms which also contains the  $K^+$  ion [23]. This demonstrates the flexibility of the (2,2) ligand which adopts conformations with various cavity sizes that can accommodate metal ions of different ionic radii. In our case, the conformation of the macrocycle is energetically favourable with torsion angles (Table 3) close to antiperiplanar ( $180^\circ$ ) or synclinal ( $60^\circ$ ) conformations. The chelating effect of the two amine groups is also important, at least with the lanthanide ions, and explains why 1:1 complexes with (2,2) are isolated for the entire rare-earth series [9], but not with the corresponding cyclic hexaether [2]. In the latter case, dinitrato complex cations have also been identified, in particular in  $[Nd(NO_3)_2(C_{12}H_{24}O_6)]_3Nd(NO_3)_6$  in which one complex cation has  $C_{2h}$  symmetry with the metal ion in the plane of the six O-atoms [6].

The mean Eu–O(ether) and Eu–O(nitrate) distances are 2.60(2) and 2.47(3) Å. One nitrate, N(3)O<sub>3</sub><sup>-</sup>, has slightly longer Eu–O distances than the other and deviates more from the ideal  $C_{2v}$  local symmetry, due to a larger steric hindrance from the organic ligand. The arrangement of the coordinating atoms around the Eu(III) ion is very irregular although it can be described as a 1:5:4 polytope (Fig. 3a) in much the same way as for the 12-crown-4 complex  $[Eu(NO_3)_3(C_8H_{16}O_4)]$  [24], albeit more distorted. The base 4-plane contains both O-atoms from N(4)O<sub>3</sub><sup>-</sup> as well as N(2) and O(3) ( $\sigma = 0.64$  Å) whilst the

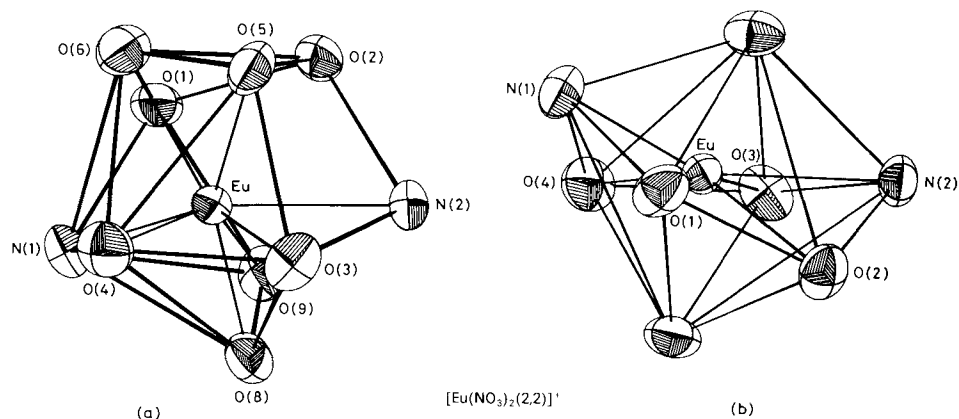


Fig. 3. (a) Coordination polyhedron around the Eu(III) ion in  $[Eu(NO_3)_2(2,2)]^-$ . (b) Same polyhedron with the nitrate ions considered as occupying one coordination site.

5-plane contains the rest of the ligand donor atoms and O(5) from the other bonded nitrate ( $\sigma = 0.78 \text{ \AA}$ ). This is capped by O(6) from the nitrate group. The site symmetry of the metal ion is approximately  $C_2$ . However, if one considers that the nitrate ions occupy only one coordination site [25] centered on the mean position of the two bonding O-atoms, the site symmetry of the Eu(III) ion approximates to  $C_{2v}$  (Fig. 3b). The effective ionic radius of the Eu(III) ion has been calculated from the Eu–O and Eu–N distances, using Shannon's definition [26] and  $r(O) = 1.31$  and  $r(N) = 1.46 \text{ \AA}$ . It amounts to  $1.21 \text{ \AA}$ , a value intermediate between those found in complexes with 12- and 15-membered polyethers,  $[Eu(NO_3)_3(C_8H_{16}O_4)]$  ( $1.18 \text{ \AA}$  [24]) and  $[Eu(NO_3)_3(C_{10}H_{20}O_5)]$  ( $1.25 \text{ \AA}$  [27]), respectively.

**Vibrational Spectra.** An earlier report concluded, on the basis of Raman and IR data, that  $Ln(NO_3)_3(2,2)$  complexes form two structurally different series,  $L_n = La - Sm$  and  $L_n = Eu - Yb$  [9]. Whilst only one type of nitrate ions are present in the former series, the vibrational spectra of the heavier lanthanides are more complex and point to the presence of three inequivalently bonded nitrates [9]. The structural results presented above prompted us to re-examine the nitrate vibrations in the Eu-complex (Table 4). The

Table 4. Nitrate Vibrations in  $[Eu(NO_3)_2(2,2)]NO_3$  [ $cm^{-1}$ ].

The assignments are based on  $C_{2v}$  and  $D_{3h}$  symmetries for bonded (b) and ionic (i) nitrate [29], respectively<sup>a</sup>).

IR	Raman	Assignment	IR	Raman	Assignment
704, 707	706, 712	$\nu_5(b)$	1395 <sup>b)</sup>	<sup>c)</sup>	$\nu_3(i)$
717vw	716vw	$\nu_4(i)$	1497, 1531	1500, 1520	$\nu_1(b)$
739, 746	740, 746	$\nu_3(b)$	1723		$\nu_2 + \nu_5(b)$ (1725) <sup>d)</sup>
809, 816 <sup>b)</sup>	810, 820 sh	$\nu_6(b)$	1740		$\nu_2 + \nu_5(b)$ (1737) <sup>d)</sup>
834 <sup>b)</sup>	832 <sup>b)</sup>	$\nu_2(i)$	1750		$\nu_2 + \nu_3(b)$ (1760)
1021, 1030	1024, 1036	$\nu_2(b)$	1760		$\nu_1 + \nu_4(i)$ (1762) <sup>d)</sup>
1045sh	1046	$\nu_1(i)$	1768		$\nu_2 + \nu_3(b)$ (1776)
1275 <sup>b)</sup> , 1292 <sup>b)</sup>	1273 <sup>b)</sup> , 1296 <sup>b)</sup>	$\nu_4(b)$			

<sup>a)</sup> vw: very weak, sh: shoulder, br.: broad.

<sup>b)</sup> These vibrations interfere with ligand vibrations.

<sup>c)</sup> Symmetry-forbidden (a broad and very weak band is present).

<sup>d)</sup> Symmetry-forbidden, but the nitrates deviate from the ideal local symmetry.

assignment of the spectra is hampered by interferences from the ligand vibrations, especially above  $1000\text{ cm}^{-1}$ . However, distinct, although weak, IR absorptions could be identified at  $717, 834, 1045,$  and  $1395\text{ cm}^{-1}$  which may be assigned to the four vibrational modes of the ionic nitrate. The  $\nu_1$  mode is formally not IR-active, but since the ionic nitrate displays positional disorder, this selection rule may be relaxed. Moreover, two distinct bands were observed for all the vibrational modes of the coordinated nitrates, in agreement with the results of the structure determination. An exact assignment of the observed vibrations to a specific nitrate group could not be made. However, the range of the  $\nu_1-\nu_4$  and  $\nu_3-\nu_5$  splittings, which are indicative of the interaction strength between the metal and the nitrate ions [28], have been determined: *ca.*  $205$  to  $255$  and  $30$  to  $40\text{ cm}^{-1}$ , which are typical values for bidentate nitrates. For  $\nu_1-\nu_4$ , a difference larger than  $15\text{ cm}^{-1}$  is observed between the two inequivalently bonded nitrates.

**Luminescence Spectra.** To help the assignment of the transitions, the excitation and emission spectra have been recorded at  $296, 77,$  and  $4\text{ K}$ . At low temperature, the intensity of the vibronic transitions decreases and the emission bands get sharper. The luminescence spectrum (Fig. 4), obtained under excitation to the  $^5D_0$  level, is dominated

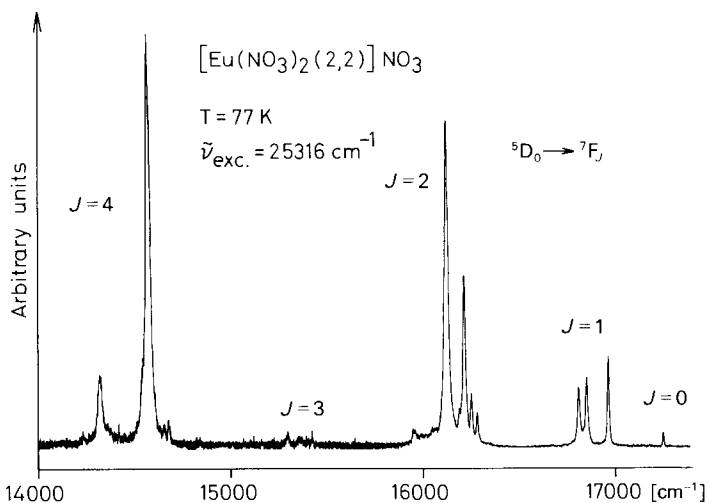


Fig. 4. Luminescence spectrum of polycrystalline  $[Eu(NO_3)_2(2,2)]NO_3$  at  $77\text{ K}$ ;  $\lambda_{exc} = 395\text{ nm}$

Table 5. Corrected Relative Intensities of the  $^5D_0 \rightarrow ^7F_J$  Transitions of  $[Eu(NO_3)_2(2,2)]NO_3$  vs. the Temperature. First column: laser-excitation on the  $^5D_0 \leftarrow ^7F_0$  transition; second column:  $\lambda_{ex} = 395\text{ nm}$ .

J	CH <sub>3</sub> CN <sup>a)</sup>		Solid state			
	300 K		300 K		77 K	4 K
0		3		5		1
1	100	100	100	100	100	100
2	430	500	460	440	420	430
3	20	50	7	9	5	10
4	350	590	440	570	420	490
5					9	6
6					42	43

<sup>a)</sup> Concentration:  $10^{-3}\text{ M}$ .

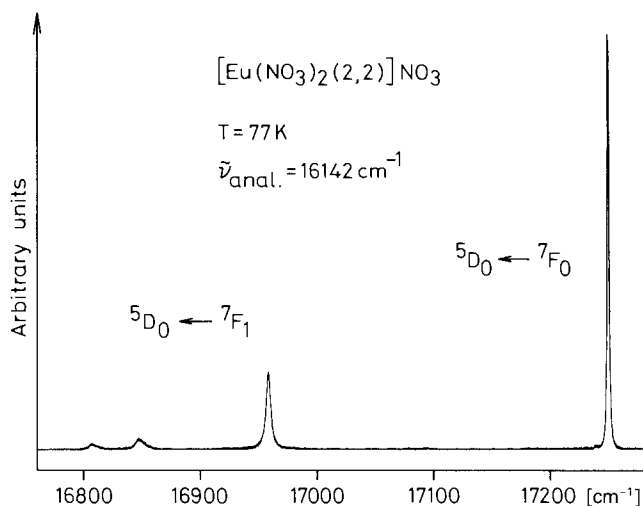


Fig. 5. Excitation spectrum of polycrystalline  $[\text{Eu}(\text{NO}_3)_2(2,2)]\text{NO}_3$  at 77 K;  $\lambda_{\text{em}} = 619.5 \text{ nm}$

by emissions from the  ${}^5\text{D}_0$  level. It is typical of a species with low symmetry: the electric dipole transitions  ${}^5\text{D}_0 \rightarrow {}^7\text{F}_2$  and  ${}^5\text{D}_0 \rightarrow {}^7\text{F}_4$  are more intense than the magnetic dipole transition  ${}^5\text{D}_0 \rightarrow {}^7\text{F}_1$ , and the latter is comprised of three components. The relative intensities of the  ${}^5\text{D}_0 \rightarrow {}^7\text{F}_j$  transitions are given in Table 5<sup>2)</sup>.

In the  ${}^5\text{D}_0 \leftarrow {}^7\text{F}_0$  region, the excitation spectrum (Fig. 5) consists of a single, sharp peak. Its width at half height varies from 5.7 to 1.9 and 1.1  $\text{cm}^{-1}$  in going from 296 to 77 and 4 K and its energy decreases from 17257 to 17251 and 17249  $\text{cm}^{-1}$ , respectively. Using a recently proposed correlation based on the energy of this transition [29], the sum of charges of the ligands bonded to the Eu(III) ion would be predicted to be  $-3.3 \pm 1.0$  for  $[\text{Eu}(\text{NO}_3)_2(2,2)]^+$ , while it is formally equal to  $-2$ . Such a difference is usually observed when the metal ion is coordinated to a cyclic polyfunctional ligand beside ionic species [30]. The energy of the  ${}^5\text{D}_0 \rightarrow {}^7\text{F}_0$  transition of similar dinitrato complex cations,  $[\text{Eu}(\text{NO}_3)_3\text{L}]^+$  with L = 18-crown-6 or 21-crown-7 ethers, is identical to that reported here [30]. In addition to the 0–0 transition, the excitation spectrum displays three bands from the  ${}^5\text{D}_0 \leftarrow {}^7\text{F}_j$  transitions, reflecting the population of the  ${}^7\text{F}_j$  level.

The emission spectra obtained under selective excitation to the  ${}^5\text{D}_0$  level allowed us to determine the energy of almost all the electronic sublevels of the  ${}^7\text{F}_j$  manifold; they are listed in Table 6. They revealed a feature that is often overlooked, but that occurs commonly with complexes containing organic ligands [31]. Whereas the  ${}^5\text{D}_0 \rightarrow {}^7\text{F}_j$  transition displays the expected three Stark components, the  ${}^5\text{D}_0 \rightarrow {}^7\text{F}_2$  transition has more than  $(2J + 1)$  components, in addition to numerous bands of vibronic origin. The width of Stark levels depends on the phonon density of states of the compound. If this density is continuous, its only effect is a broadening of the electronic level, and the classical theory of crystal field splitting may be used to interpret the number of components of the observed transitions. On the contrary, if the phonon density of states is resolved into

<sup>2)</sup> A listing of all observed transitions and figures of each of the  ${}^5\text{D}_0 \rightarrow {}^7\text{F}_j$  transition is available upon request from J.-C. B.

Table 6. Energy Levels [ $\text{cm}^{-1}$ ] of the Eu(III) Ion in  $[\text{Eu}(\text{NO}_3)_2(2,2)]\text{NO}_3$ , at 4 K, from Excitation and Emission Spectra

${}^7\text{F}_0$	0	${}^7\text{F}_3$	1708 1829	${}^7\text{F}_4$	2573 2596 2648	${}^7\text{F}_5$	3754 3809 3854	${}^7\text{F}_6$	4858 4947 4985	${}^5\text{D}_0$	17249
${}^7\text{F}_1$	286 397 442		1850 1879 1887 1895		2673 2683 2697		3880 3901 3908		5001 5036 5050	${}^5\text{D}_1$	18975 <sup>b)</sup> 18990 <sup>b)</sup> 19012 <sup>b)</sup>
${}^7\text{F}_2$	967 998 1035 <sup>a)</sup> 1062? 1129 <sup>a)</sup>		1956		2709 2927 2933		3914 3937 3985		5055 5106 5155	${}^5\text{D}_2$	21422 <sup>b)</sup> 21447 <sup>b)</sup> 21465 <sup>b)</sup>
							4048 4108		5166 5198 5209		

<sup>a)</sup> Average of levels split by resonance effects (see text).

<sup>b)</sup> At 20 K.

sharp peaks, splittings may occur from resonance effect with the electronic sub-levels [24]. The  ${}^5\text{D}_0 \rightarrow {}^7\text{F}_2$  transition occurs between *ca.* 950 and 1150  $\text{cm}^{-1}$ , in a range corresponding to the energy of both nitrate and ligand vibrations (Fig. 6). Resonance phenomena may then easily be present and the emission spectrum contains satellite lines. For instance, the two sharp components at 616.63 and 616.81 nm correspond to energy differences of 1032 and 1037  $\text{cm}^{-1}$ , with respect to the  ${}^7\text{F}_0$  level. This doublet probably arises from an interaction between one  ${}^7\text{F}_2$  sublevel and the nitrate vibration at 1036  $\text{cm}^{-1}$ . Similar satellites are not observed for the other  ${}^5\text{D}_0 \rightarrow {}^7\text{F}_j$  transitions which do not overlap with a

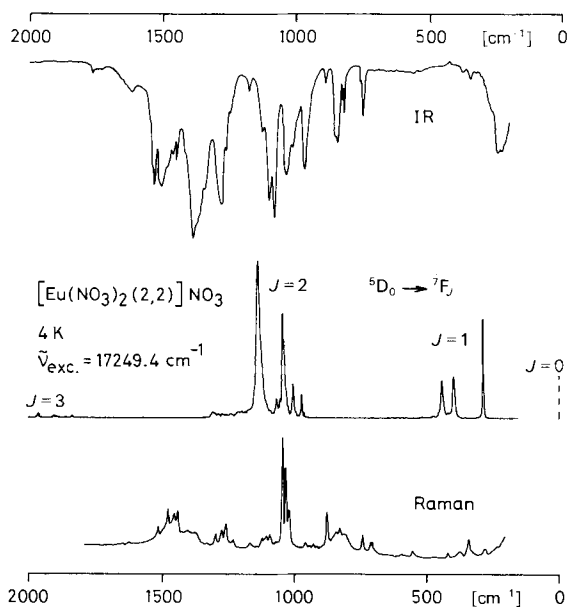


Fig. 6. IR (top) and Raman (bottom) spectra of  $[\text{Eu}(\text{NO}_3)_2(2,2)]\text{NO}_3$  in correlation with part of its luminescence spectrum at 4 K. The excitation energy ( $17249 \text{ cm}^{-1}$ ) is taken as origin.



sharp phonon density distribution. Despite these effects, the luminescence spectra remain useful to characterize a specific species in compounds possessing several different chemical environments for the metal ion, and to determine their site symmetry [30] [32].

**Solution Study.** The emission spectra of  $10^{-3}$  M solutions in anhydrous MeCN closely resemble those of the polycrystalline samples. They are less well-resolved, but the barycenters of the transitions are almost the same as in the solid state. The only differences lie in slightly different intensity ratios (Table 5) and in a broadened  ${}^5D_0 \rightarrow {}^7F_0$  transition at  $17255\text{ cm}^{-1}$  (width at half height:  $11\text{ cm}^{-1}$ ), which displays a weak shoulder at  $17248\text{ cm}^{-1}$ . Selective excitations on the maximum and on the shoulder yielded essentially the same luminescence spectra, but for an intensity inversion of two components of the  ${}^5D_0 \rightarrow {}^7F_2$  transition. We, therefore, conclude that the complex cation  $[\text{Eu}(\text{NO}_3)_2(2,2)]^+$  is probably present in these solutions, as has been established for solutions containing the 18-crown-6 complex [7], and that it is in equilibrium with a small amount of another complex species containing a different number of coordinated nitrate ions. In agreement with this, the molar conductivity of a  $10^{-3}$  M solution is  $135\ \Omega^{-1}\cdot\text{cm}^2\cdot\text{mol}^{-1}$  at 298 K, within the range for 1:1 electrolytes ( $120\text{--}160\ \Omega^{-1}\cdot\text{cm}^2\cdot\text{mol}^{-1}$ ) [33]. The addition of up to 40 molecules of  $\text{H}_2\text{O}$  per Eu(III) ion only slightly modified the conductivity ( $143\ \Omega^{-1}\cdot\text{cm}^2\cdot\text{mol}^{-1}$ ).

**Conclusion.** – Although common in complexes with a ligand to metal ratio larger than 1 (3:2 or 4:3), cationic complex species  $[\text{LnX}_2\text{L}]^+$  rarely occur in 1:1 coronates or cryptates [2]. This study reports the second example of such a cation, the other being a dichloro complex of 18-crown-6 ether with Gd(III) [8]. The formation of this dinitrato cation may be traced back to the presence of the two amine groups in (2,2), which confer a greater flexibility to the cycle. Additional stabilization through the formation of stable pentakis- or hexakis(nitrato) complexes is, therefore, not needed, and the compound exists as a 1:1 coronate.

This study also demonstrates that, despite spectral interference by the macrocycle, the vibrational spectra show the presence of free and bonded nitrate ions. Furthermore, the luminescence spectra provide an example of the interactions occurring between the phonon density of states of the complex and the electronic sublevels of the Eu(III) ion, leading to the appearance of satellite lines.

Support from the *Swiss National Science Foundation* is gratefully acknowledged. We thank the *Fondation Herbet* (Lausanne) for the gift of the spectroscopic equipment, Prof. D. *Schwarzenbach* for allowing us to use his computer programme on soft constraints, Dr. G.-O. *Pradervand* for his help in recording the luminescence spectra, and Mrs. B. *Reuge* for technical assistance.

#### REFERENCES

- [1] J.-C. G. Bünzli, A. Giorgetti, *Inorg. Chim. Acta* **1985**, *110*, 225.
- [2] J.-C. G. Bünzli, D. Wessner, *Coord. Chem. Rev.* **1984**, *60*, 191.
- [3] W. DeW. Horrocks, Jr., M. Albin, *Progr. Inorg. Chem.* **1984**, *31*, 1.
- [4] C. Pascard, C. Riche, M. Cesario, F. Kotzyba-Hibert, J.-M. Lehn, *J. Chem. Soc., Chem. Commun.* **1982**, 557.
- [5] D. Plancherel, J.-C. G. Bünzli, J.-M. Lehn, in 'New Frontiers in Rare Earth Science and Applications', Eds. Xu Guangxian and Xiao Jimei, Science Press, Beijing, 1985, Vol. 1, pp. 131–133.
- [6] J.-C. G. Bünzli, B. Klein, D. Wessner, K. J. Schenk, G. Chapuis, G. Bombieri, G. de Paoli, *Inorg. Chim. Acta* **1981**, *54*, L43.
- [7] D. H. Metcalf, R. G. Ghirardelli, R. A. Palmer, *Inorg. Chem.* **1985**, *24*, 634.

- [8] E. Forsellini, F. Benetollo, G. Bombieri, A. Cassol, G. de Paoli, *Inorg. Chim. Acta* **1985**, *109*, 167.
- [9] J.-F. Desreux, A. Renard, G. Duyckaerts, *J. Inorg. Nucl. Chem.* **1977**, *39*, 1587.
- [10] J.-C. G. Bünzli, B. Klein, G.-O. Pradervand, P. Porcher, *Inorg. Chem.* **1983**, *22*, 3763.
- [11] a) P. Blessing, P. Coopens, P. Becker, *J. Appl. Crystallogr.* **1972**, 488; b) D. Schwarzenbach, Abstr. 4th Eur. Cryst. Meeting 1977, 1-20.
- [12] J. D. Dunitz, M. Dobler, P. Seiler, R. P. Phizackerley, *Acta Crystallogr., Sect. B* **1974**, *30*, 2733.
- [13] J. D. Dunitz, P. Seiler, *Acta Crystallogr., Sect. B* **1973**, *29*, 589.
- [14] D. Schwarzenbach, personal communication.
- [15] J. M. Stewart, Technical Report TR-192, Computer Science Centre, University of Maryland, 1972.
- [16] D. T. Cromer, D. J. Liberman, *J. Chem. Phys.* **1970**, *53*, 1891.
- [17] D. T. Cromer, J. B. Mann, *Acta Crystallogr., Sect. A* **1968**, *24*, 321.
- [18] M. Herceg, R. Weiss, *Bull. Soc. Chim. Fr.* **1972**, 549.
- [19] J. D. J. Backer-Dirks, J. E. Cooke, A. M. R. Galas, J. S. Ghotra, C. J. Gray, F. A. Hart, M. B. Hursthouse, *J. Chem. Soc., Dalton Trans.* **1980**, 2191.
- [20] J.-C. G. Bünzli, B. Klein, D. Wessner, *Inorg. Chim. Acta* **1980**, *44*, L147.
- [21] M. E. Harman, F. A. Hart, M. B. Hursthouse, G. P. Moss, P. R. Raithby, *J. Chem. Soc., Chem. Commun.* **1976**, 396.
- [22] a) L.-A. Malmsten, *Acta Crystallogr., Sect. B* **1979**, *35*, 1702; b) B. Metz, R. Weiss, *ibid.* **1973**, *29*, 1088.
- [23] D. Moras, B. Metz, M. Herceg, R. Weiss, *Bull. Soc. Chim. Fr.* **1972**, 551.
- [24] J.-C. G. Bünzli, B. Klein, D. Wessner, N. W. Alcock, *Inorg. Chim. Acta* **1982**, *59*, 269.
- [25] J. G. Bergmann, Jr., F. A. Cotton, *Inorg. Chem.* **1966**, *5*, 1208.
- [26] R. D. Shannon, *Acta Crystallogr., Sect. A* **1976**, *32*, 751.
- [27] J.-C. G. Bünzli, B. Klein, G. Chapuis, K. J. Schenk, *Inorg. Chem.* **1982**, *21*, 808.
- [28] H. Brintzinger, R. E. Hester, *Inorg. Chem.* **1966**, 5,980.
- [29] M. Albin, W. DeW. Horrocks, Jr., *Inorg. Chem.* **1985**, *24*, 895.
- [30] J.-C. G. Bünzli, G.-O. Pradervand, unpublished results.
- [31] P. Caro, O. K. Moune, F. Antic-Fidancev, M. Lemaitre-Blaise, *J. Less-Common Met.* **1985**, *112*, 153.
- [32] M. Albin, A. C. Goldstone, A. Sommerville-Withers, W. DeW. Horrocks, Jr., *Inorg. Chem.* **1983**, *22*, 3182.
- [33] W. J. Geary, *Coord. Chem. Rev.* **1971**, *7*, 81.